

Numerical modeling of the formation of the screening charge near the thundercloud boundaries and its impact on the initiation and early stages of development of blue jets

Jeremy A. Riousset and Victor P. Pasko

CSSL Laboratory, The Pennsylvania State University, University Park,
Pennsylvania, USA.

Paul R. Krehbiel, Ronald J. Thomas and William Rison

New Mexico Institute of Mining and Technology, Socorro, New Mexico, USA

Mark A. Stanley

114 Mesa Verde Road, Jemez Springs, New Mexico, 87025, USA.

(sparky@mark-stanley.name)

A new 2-D axisymmetric model of Maxwellian relaxation of the atmosphere accounting for time dependent conduction currents and screening charges formed under the influence of the thundercloud charge sources is used in conjunction with *Riousset et al.*'s [2007] model of lightning discharge to demonstrate how realistic cloud dynamics leads to the development of blue jets. Particular attention is given to a time dependent numerical modeling of the screening charges near the boundary and to the discussion of the role of these screening charges in local enhancement of the electric field, leading to the charge configuration facilitating the initiation of blue jets, as originally proposed in [*Krehbiel et al.*, 2008].

J. A. Riousset and V. P. Pasko, Department of Electrical Engineering, Communications and Space Sciences Laboratory (CSSL), The Pennsylvania State University, 211B Electrical Engineering East, University Park, PA 16802, USA. (riousset@psu.edu; vpasko@psu.edu)

P. R. Krehbiel, Physics Department, New Mexico Institute of Mining and Technology, Socorro, NM 87801, USA. (krehbiel@ibis.nmt.edu)

W. Rison and R. J. Thomas, Electrical Engineering Department, New Mexico Institute of Mining and Technology, Socorro, NM 87801, USA. (rison@ee.nmt.edu; thomas@nmt.edu)

M. A. Stanley, 114 Mesa Verde Road, Jemez Springs, NM, 87025, USA. (sparky@mark-stanley.name)

1. Introduction

Krehbiel et al. [2008] demonstrated how charge imbalances in the thundercloud lead to the development of various lightning discharges, including upward directed electrical discharges, so-called blue jets [*Wescott et al.*, 1995; *Sentman and Wescott*, 1995; *Boeck et al.*, 1995; *Wescott et al.*, 2001] and gigantic jets [*Pasko et al.*, 2002; *Su et al.*, 2003; *van der Velde et al.*, 2007]. In addition to local and global thundercloud charge imbalances created by intracloud lightning or cloud-to-ground discharges prior to initiation of jet discharges, *Krehbiel et al.* [2008] also emphasized the role of the screening charge forming around thundercloud boundaries in the development of both kinds of jets. Indeed, the screening charges can reduce the net charge content in the upper charge region of a tall thundercloud because of the variation in atmospheric conductivity as first suggested by *Wilson* [1921]. It can also magnify the local electric field near the cloud boundary through the formation of an extra charge layer. This last hypothesis was initially explored with *Krehbiel et al.*'s [2004] model to demonstrate how the enhanced electric field at the top of the thunderstorm explains the development of blue jets and was further investigated with an evolution of this model in [*Krehbiel et al.*, 2008, Supplementary Information].

In this work, we use a new two-dimensional axisymmetric model to demonstrate how the Maxwellian relaxation of the atmosphere [e.g., *Pasko et al.*, 1997] due variations in the conductivity in and nearby the thundercloud dynamically leads to the formation of the screening charges enhancing the electric field near the cloud top boundary. It is believed that jet discharges are initiated on a conventional leader

form [Krehbiel *et al.*, 2008] and the initial leader development of the jet discharge is modeled using the 3-D Cartesian model of lightning discharge described in [Riousset *et al.*, 2007] and first applied to the study of jet discharges in [Krehbiel *et al.*, 2008].

Classical, normally electrified thunderstorms have a dominant negative charge region (N) adjacent to a comparable upper positive charge region (P) above, and a smaller lower positive charge region beneath (LP) [e.g., Williams, 1989] pictured in Figure 1 by blue and red rectangles marked N, P and LP, respectively. The storm charges and electric fields build up with time as a result of charging currents, believed to be precipitation driven [e.g., Williams, 1989], until a breakdown threshold is reached. At this point, bidirectional discharges occur, producing different lightning types depending on where the triggering occurs first [Krehbiel *et al.*, 2008]. These discharges reduce the net charges within the charge regions. These rearrangements of charge provoke the formation of so-called *Greifinger and Greifinger's* [1976] boundaries, which represent charges dynamically formed in the conducting atmosphere due to time variation of thundercloud source charges. In an atmosphere with conductivity increasing with altitude a *Greifinger and Greifinger's* [1976] boundary separates the regions dominated by conduction current below it and displacement current above it. The location of this boundary depends on the dynamics of the thunderstorm in the troposphere. Fast charge rearrangements due to any discharge result in downward moving boundaries while slow charge rearrangements due to charge build up in the thunderstorm lead to the formation of a screening charge usually accumulating at the boundary of the thundercloud [e.g., Pasko and George, 2002]. The so-created

screening layer enhances the electric field locally between the upper positive charge layer and the screening charge, permitting the initiation of blue jet near the cloud top [Krehbiel *et al.*, 2008]. It is believed that jets are initiated as regular lightning leader channels, which then convert to non-thermal, streamer zone dominated form at higher altitudes [Petrov and Petrova, 1999].

2. Model Formulation

The model developed for the purpose of simulating the time dynamics of the thundercloud in a conducting atmosphere employs a 2-D axisymmetric domain. The domain is discretized using equidistant grids spaced by 500 m and 250 m in the r - and z -directions, respectively. The ground altitude and other parameters for the model case presented in this paper are summarized in Table 1 and Figure 1.

The following system of equations is used in the present study to model the thundercloud dynamics:

$$\vec{\nabla}^2 \phi = -\frac{\rho + \rho_s}{\varepsilon_0} \quad (1)$$

$$\frac{\partial \rho}{\partial t} - \vec{\nabla} \sigma \cdot \vec{\nabla} \phi = -\sigma \frac{\rho + \rho_s}{\varepsilon_0} \quad (2)$$

where ϕ , ρ_s , ρ , σ , ε_0 refer to the total electric potential, source charge density, induced charge density, atmospheric electric conductivity, and permittivity of free space, respectively. The conduction current \vec{J} has been expressed as $\vec{J} = -\sigma \vec{\nabla} \phi$ to obtain the continuity equation in the form given by (2).

The thundercloud is defined as a classic tripolar charge structure [e.g., Williams, 1989] enclosed in a dielectric cylinder of radius r_c and vertical extent z_c (Table 2)

representing the limits of the cloud. The tripole is placed above a perfectly electrically conducting (PEC) flat ground plane at the altitude $z=z_{\text{gnd}}$. The charge regions are modeled as axisymmetric cylinders at altitudes z_N, z_P, z_{LP} with radii R_N, R_P, R_{LP} , depths d_N, d_P, d_{LP} , and net charge contents Q_N, Q_P, Q_{LP} , respectively.

The conductivity σ at any location in the simulation domain is given by:

$$\sigma(r, z) = \underbrace{\sigma_a e^{\frac{z+z_{\text{gnd}}}{z_a}}}_{\text{(I)}} \underbrace{\left(1 - \frac{1 - \tanh\left(\frac{r-r_c}{\alpha}\right)}{2} \times \frac{1 - \tanh\left(\frac{z-z_c}{\alpha}\right)}{2} \right)}_{\text{(II)}} \quad (3)$$

where α refers to the thickness of the conductivity transition region between the cloud interior and the surrounding clear air. The conductivity outside the cloud increases exponentially with altitude z (term (I) in (3)) with an altitude scaling factor $z_a=6$ km and a conductivity at sea level $\sigma_a=5 \times 10^{-14}$ S/m [e.g., *Pasko et al.*, 1997]. Measurements of the conductivity σ within the thundercloud are scarce [*MacGorman and Rust*, 1998, p. 171 and references therein]. In the present study, we adopted the hypothesis of a low conductivity [e.g., *MacGorman and Rust*, 1998, pp. 170–172; *Rakov and Uman*, 2003, p. 91] and set it equal to zero. Term (II) in (3) approaches zero in the cylinder defined by $z < z_c$ and $r < r_c$ and 1 outside, with a smooth transition at the boundary with a characteristic width α (see Table 2).

With the expression of σ given by (3), we can solve the system (1)–(2). Poisson equation (1) is solved using a red-black parallel Successive Overrelaxation Method (SOR) [*Niethammer*, 1989; *Zhang et al.*, 2006], while the continuity equation is solved using a parallel Lax scheme [*Potter*, 1973, pp. 57 and 67]. The system (1)–(2) is solved with time step $\Delta t=0.4$ ms, so that at all time moments during the simulations

and at all locations in the simulation domain, the time step remains smaller than the relaxation time $\tau_{\sigma}=\varepsilon_0/\sigma(r, z)$.

The thundercloud source charge density ρ_s is brought by the loading currents $I_1=5$ A and $I_2=-1$ A and uniformly distributed within the charge regions specified in Table 1 and shown on Figure 1. To model the bulk effect of lightning occurrence on the thundercloud dynamics, three forms of discharges are accounted for: (1) cloud-to-ground discharge (CG), which reduces by 50% the net charge contents of LP- and N-layers, (2) intracloud discharge (IC), which yields a reduction of $\min(|Q_N|, |Q_P|)/2$ of the net charge in the N- and P-layers, and (3) blue jet discharge (BJ), which are simulated by a reduction of 50% of the screening charge and net charge in the P-layer [Krehbiel *et al.*, 2004]. A discharge occurs when the electric field exceeds a predefined electric field threshold for initiation and propagation of positive and negative leaders $E_{\text{th}}^{\pm}=2.16\times N(z+z_{\text{gnd}})/N_0$ kV \cdot cm $^{-1}$, with $N(z)$ and N_0 being the neutral density at altitude z and at sea level, respectively [e.g., Rioussset *et al.*, 2007, and references therein]. This permits to discriminate the electric discharges depending on their initiation altitudes. Thus, a charge configuration resulting in the electric field propagation threshold being exceeded between the LP- and N-layers leads to a CG. If initiation occurs between the N- and P-layers, then IC occurs, and finally if the initial breakdown occurs above the P-layer, then we assume the occurrence of a jet event.

During model calculations, the side and top boundaries are maintained at ground potential (Dirichlet boundary conditions). This hypothesis is fully justified for the

ground and ionospheric boundaries [e.g., *Pasko et al.*, 1997] and introduces an error <10% on the side boundary, decreasing as we get closer to the center of the simulation domain at $r=0$, i.e., in the region of primary interest.

At the moment of jet initiation, a “still picture” of the charge configuration is taken and then converted to 3-D Cartesian coordinates to be used for simulation of the discharge itself. Modeling of the jet employs the stochastic model described in [*Riousset et al.*, 2007; *Krehbiel et al.*, 2008] in a domain enclosing the cloud and its nearest surroundings (see Tables 1 and 2). The use of a reduced simulation domain requires the use of the Dirichlet open boundary conditions described in [*Riousset et al.*, 2007]. Comparison of the electric fields at $r=0$ shows very good agreement between the 2-D cylindrically axisymmetric and 3-D Cartesian models.

3. Results

In this section we present the results of a typical simulation run leading to a blue jet event.

Figure 1 shows the atmospheric conductivity profile (equation (3)) used in thunderstorm dynamics modeling. We note that for clarity of presentation Figure 1 only shows a small part of the large 62.5 km×72.5 km simulation domain. The dashed green lines represent the lightning initiation and propagation threshold E_{th}^{\pm} while the solid blue line shows the electric field at the time of the initiation of the jet. The initiation threshold is crossed at $z=10.75$ km, above the P-layer allowing for the development of the jet. The vertical arrows represent the loading currents I_1 and I_2 .

Figure 2 represents the evolution of net charges contained in the LP- (dashed red line), N- (solid blue line) and P-layers (solid red line). The screening charge at the top of the cloud is calculated as: $\iiint_V \rho(\vec{r})dV$ where $\rho(\vec{r})$ is the induced charge density introduced in (1) and (2) at the location \vec{r} and V the volume above the P-layer. The evolution of this quantity in Figure 2 is shown with a dashed blue line. Finally, the total charge in the thundercloud calculated as the sum of the four previous values is shown using a solid black line. The sudden jumps in the curves correspond to the occurrence of discharge events (CG, IC or BJ).

Figure 3a shows the total charge density $\rho_t = \rho_s + \rho$ in the 2-D simulation domain at the instant of initiation of the jet, while Figure 3b shows the magnitude of the electric field at the same instant of time. Panel (a) reveals the location of the upper screening charge. Panel (c) shows the model jet discharge developing under the conditions given by the 2-D model. Initiation occurs at $z=10.75$ km and the discharge then develops bidirectionally from that point on, crosses the screening charge at the top of the cloud, and further develops towards the ionosphere. The simulation is stopped when the discharge exits the simulation domain (through the $y=0$ boundary in the present situation, topping at ~ 15 km). It is expected [e.g., *Petrov and Petrova, 1999; Pasko and George, 2002; Krehbiel et al., 2008*] that the streamer corona of the thermalized leader section of the jet would expand up to the altitude of the *Greifinger and Greifinger's* [1976] boundary, consistent with published observations of blue jets [e.g., *Wescott et al., 1995; Sentman and Wescott, 1995; Boeck et al., 1995; Wescott et al., 2001*].

4. Discussion

The conductivity of the moist air within the cloud is decreased due to ion attachment to hydrometeors [Rakov and Uman, 2003, p. 91] compared to that of the surrounding dry clear air. This results in an abrupt change in conductivity near the cloud boundary (Figure 1). The location and thickness of this transition from lower to higher conductivity depends on factors like overturning [e.g., Holton, 2004, p. 377] and maturity of the storm [e.g., Wallace and Hobbs, 1973, p. 351]. Strong overturning pushes the transition within the cloud boundaries favoring mixing of the screening charge with the cloud upper charge layer, yielding possible strong imbalance between the N- and P-layers, while weak overturning limits the mixing of the screening charge with the cloud charge layers. In the latter case, the screening charge accumulates near the cloud boundaries, allowing for the formation of an extra charge layer at the cloud top boundary as seen in Figures 3a and 3c. Figure 3a also shows the formation of lateral screening charge around the N-layer providing the lateral charge necessary to develop ‘bolt-from-the-blue’ discharges [e.g., Rison *et al.*, 1999] as modeled in [Krehbiel *et al.*, 2008].

The so-created dipolar structure at the cloud upper boundary results in a gradual local enhancement of the electric field (as screening charge accumulates above the cloud), ultimately resulting in an initiation of jet discharge around ~ 11 km altitude after ~ 62 s. Figure 2 shows that at this instant, Q_P is about ten times larger than Q_{SC} . This charge imbalance forces the lightning to find a path outside the cloud in a form of upward jet discharge [Krehbiel *et al.*, 2008]. Additionally, the quasi-

exponential decrease of the electric field threshold with altitude (Figure 1) favors upward propagation leading to the jet event modeled in Figure 3c. The history of the thunderstorm before the occurrence of the jet (Figure 2) reveals the occurrence of numerous “classic” discharges (of CG or IC types). The dominant current I_1 charges both N- and P-layers. Besides, the current I_2 also loads the N-layer, contributing to the occurrence of IC discharges. The current I_2 controls the frequency of occurrence of CG discharges by defining the rate of charge accumulation in the LP-layer. The low conductivity of both dry and moist air at low altitudes limits the effects of the screening charge on the development of CG discharges, confirming the earlier simulation results presented in [Krehbiel *et al.*, 2008]. The succession of IC at $t \simeq 40, 44, 48, 52$ and 56 s weakens the N- and P-layer preventing the occurrence of an IC at $t=62$ s, while the CG occurring ~ 5 s before the jet increases the excess of positive charge in the cloud, leaving the development of a BJ as only allowed discharge mechanism, consistent with the theory developed by Krehbiel *et al.* [2008]. We note that the initiation of the jet discharge at $t=62$ s is also strongly influenced by gradual accumulation and growth of the screening charge Q_{SC} above the cloud (see Figures 2 and 3c).

Observations of blue jets [Wescott *et al.*, 1995; Sentman and Wescott, 1995; Boeck *et al.*, 1995; Wescott *et al.*, 2001] revealed a fine filamentary structure later identified as streamer channels [e.g., Pasko and George, 2002]. The development of such channels without a lightning leader would require unrealistic amount of charges near the cloud top [Pasko and George, 2002]. The modeling scenario reported in the

present work shows how a lightning leader can propagate from the cloud upward, providing a stem above the thundercloud ($z=15$ km or higher) for development of the streamer corona up to the lower ionosphere, quantitatively demonstrating the idea first expressed by *Petrov and Petrova* [1999] and further developed in [*Krehbiel et al.*, 2008].

5. Conclusion

In this paper, we introduced a new 2-D axisymmetric model of the Maxwellian relaxation of the atmosphere. The model was applied in conjunction with *Riousset et al.*'s [2007] model of lightning to develop a consistent scenario leading to the development of blue jet discharges. Our paper demonstrates how prior occurrence of IC discharges can sufficiently weaken the N- and P-layers to prevent occurrence of an IC at the time of jet initiation while a CG developing several seconds before the jet events enhances the excess of positive charge in the cloud by bringing negative charge to the ground. The screening charge gradually developing at the cloud top leads to breakdown initiation near the cloud upper boundary, but is insufficient to contain the lightning leader channel within the cloud resulting in occurrence of upward propagating blue jet events.

Acknowledgments. This research was supported by the United States National Science Foundation under grant ATM-0652148 to the Pennsylvania State University.

References

- Boeck, W. L., O. H. Vaughan, R. J. Blakeslee, B. Vonnegut, M. Brook, and J. McKune (1995), Observations of lightning in the stratosphere, *J. Geophys. Res.*, *100*, 1465.
- Greifinger, C., and P. Greifinger (1976), Transient ULF electric and magnetic fields following a lightning discharge, *J. Geophys. Res.*, *81*(13), 2237–2247.
- Holton, J. R. (2004), *An Introduction to Dynamic Meteorology, International Geophysics*, vol. 88, 4th ed., Academic Press, New York, NY.
- Krehbiel, P., W. Rison, R. Thomas, T. Marshall, M. Stolzenburg, W. Winn, and S. Hunyady (2004), Thunderstorm charge studies using a simple cylindrical charge model, electric field measurements, and lightning mapping observations, *Eos Trans. AGU*, *85*(47), Fall Meet. Suppl., Abstract AE23A-0843.
- Krehbiel, P. R., J. A. Rioussset, V. P. Pasko, R. J. Thomas, W. Rison, M. A. Stanley, and H. E. Edens (2008), Upward Electrical Discharges from Thunderstorms, *Nature Geoscience*, *1*(4), 233–237, doi:10.1038/ngeo162.
- MacGorman, D. R., and W. D. Rust (1998), *The Electrical Nature of Storms*, Oxford Univ. Press, New York, NY.
- Niethammer, W. (1989), The SOR method on parallel computers, *Numer. Math.*, *56*, 247–254.
- Pasko, V. P., and J. J. George (2002), Three-dimensional modeling of blue jets and blue starters, *J. Geophys. Res.*, *107*(A12), 1458, doi:10.1029/2002JA009473.

- Pasko, V. P., U. S. Inan, T. F. Bell, and Y. N. Taranenکو (1997), Sprites produced by quasi-electrostatic heating and ionization in the lower ionosphere, *J. Geophys. Res.*, *102*(A3), 4529–4561, doi:10.1029/96JA03528.
- Pasko, V. P., M. A. Stanley, J. D. Matthews, U. S. Inan, and T. G. Wood (2002), Electrical discharge from a thundercloud top to the lower ionosphere, *Nature*, *416*, 152–154, doi:10.1038/416152a.
- Petrov, N. I., and G. N. Petrova (1999), Physical mechanisms for the development of lightning discharges between a thundercloud and the ionosphere, *Tech. Phys.*, *44*, 472–475.
- Potter, D. (1973), *Computational Physics*, John Wiley & Sons, Inc., New York, NY.
- Rakov, V. A., and M. A. Uman (2003), *Lightning: Physics and Effects*, Cambridge Univ. Press, Cambridge, U.K.; New York.
- Riousset, J. A., V. P. Pasko, P. R. Krehbiel, R. J. Thomas, and W. Rison (2007), Three-dimensional fractal modeling of intracloud lightning discharge in a New Mexico thunderstorm and comparison with lightning mapping observations, *J. Geophys. Res.*, *112*(D15203), doi:10.1029/2006JD007621.
- Rison, W., R. J. Thomas, P. R. Krehbiel, T. Hamlin, and J. Harlin (1999), A GPS-based three-dimensional lightning mapping system: Initial observations in central New Mexico, *Geophys. Res. Lett.*, *26*(23), 3573–3576, doi:10.1029/1999GL010856.
- Sentman, D. D., and E. M. Wescott (1995), Red sprites and blue jets: Thunderstorm-excited optical emissions in the stratosphere, mesosphere, and ionosphere, *Phys. Plasmas*, *2*(6), 2514–2522, doi:10.1063/1.871213.

- Su, H. T., R. R. Hsu, A. B. Chen, Y. C. Wang, W. S. Hsiao, W. C. Lai, L. C. Lee, M. Sato, and H. Fukunishi (2003), Gigantic jets between a thundercloud and the ionosphere, *Nature*, *423*, 974–976, doi:10.1038/nature01759.
- van der Velde, O. A., W. A. Lyons, T. E. Nelson, S. A. Cummer, J. Li, and J. Bunnell (2007), Analysis of the first gigantic jet recorded over continental north america, *J. Geophys. Res.*, *112*, D20104, doi:10.1029/2007JD008575.
- Wallace, J. M., and P. V. Hobbs (1973), *Atmospheric Science, An Introductory Survey, International Geophysics*, vol. 92, 2nd ed., Academic Press, New York, NY.
- Wescott, E. M., D. Sentman, D. Osborne, D. Hampton, and M. Heavner (1995), Preliminary results from the Sprites94 aircraft campaign: 2. Blue jets, *Geophys. Res. Lett.*, *22*(10), 1209–1212.
- Wescott, E. M., D. Sentman, H. C. Stenbaek-Nielsen, P. Huet, M. J. Heavner, and D. R. Moudry (2001), New evidence for the brightness and ionization of blue jets and blue starters, *J. Geophys. Res.*, *106*(A10), 21,549–21,554, doi:10.1029/2000JA000429.
- Williams, E. R. (1989), The tripolar structure of thunderstorms, *J. Geophys. Res.*, *94*(D11), 13,151–13,167.
- Wilson, C. T. R. (1921), Investigations on lightning discharges and on the electric field of thunderstorms, *Phys. Trans. Roy. Soc. London A*, *221*, 73–115.
- Zhang, C., H. Lan, Y. Pe, and B. D. Estrade (2006), Parallel SOR iterative algorithms and performance evaluation on a Linux cluster, *Nav. Res. Lab. Rep.*, *0603207N*, 20060619021.

Table 1. Parameters used in the simulations.

Name	Symbol	Unit	Value
Ground altitude	z_{gnd}	(km)	3
2-D domain dimensions ^a	L_r	(km)	62.5
	L_z	(km)	72.5
3-D domain dimensions ^b	L_x	(km)	12.5
	L_y	(km)	12.5
	L_z	(km)	18.0

^a 2-D axisymmetric domain

^b 3-D Cartesian domain

Table 2. Geometrical parameters of the thundercloud.

Name		Symbol	Unit	Value
<i>Charge layer geometry</i>				
Lower positive	altitude ^a	z_{LP}	(km)	2.0
	radius	R_{LP}	(km)	1.5
	depth	d_{LP}	(km)	1.5
Central negative	altitude ^a	z_N	(km)	3.75
	radius	R_N	(km)	3.0
	depth	d_N	(km)	1.5
Upper positive	altitude ^a	z_P	(km)	6.75
	radius	R_P	(km)	4.0
	depth	d_P	(km)	1.5
<i>Cloud boundaries</i>				
Radius		r_c	(km)	4
Height ^a		z_c	(km)	10
Boundary thickness		α	(km)	0.3

^a altitude above ground level

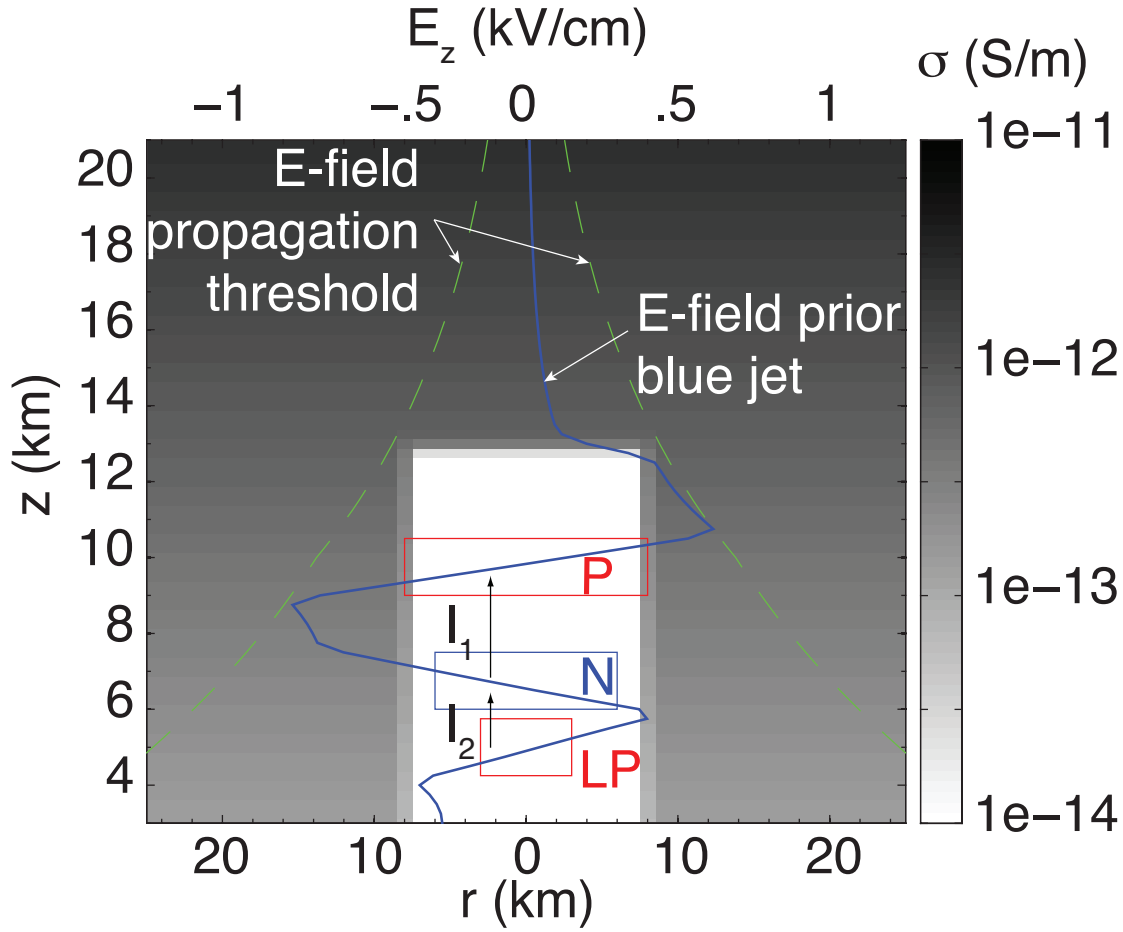


Figure 1. Geometry employed for the simulation of blue jets and the conductivity distribution inside and nearby the cloud. The background gray scale variation shows the atmospheric conductivity σ . The use of hyperbolic tangent functions in equation (3) avoids sharp cloud boundaries. Dashed green lines represent the model electric field threshold E_{th}^{\pm} for lightning initiation. The solid blue line represents the electric field at $r=0$ prior to the development of the jet. The solid rectangles marked LP, N and P depict the altitude and dimensions of the lower positive, central negative and upper positive thundercloud charge regions, respectively (Tables 1 and 2). The vertical arrows represent the loading currents I_1 and I_2 .

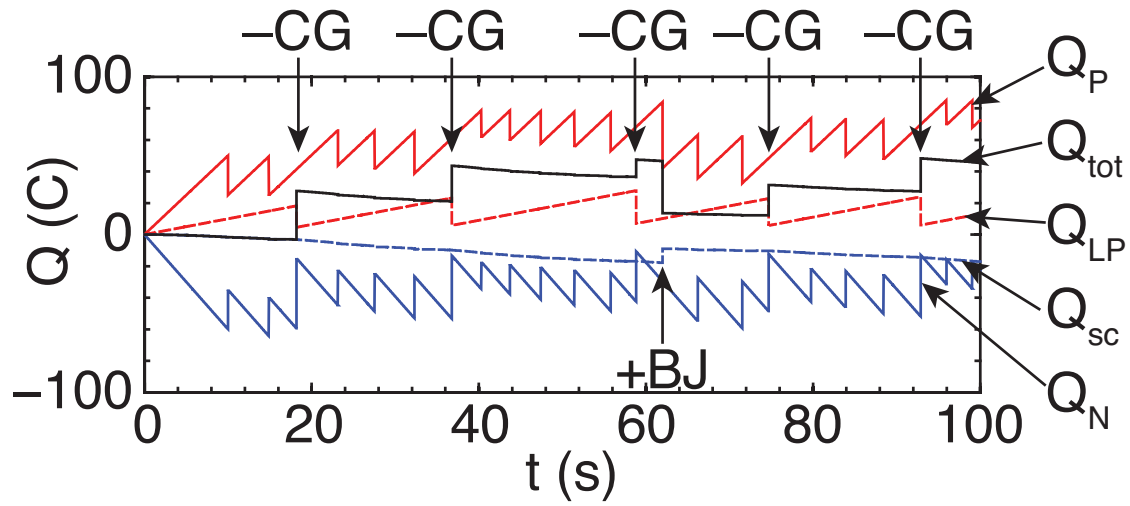


Figure 2. Model-calculated temporal variation of the storm charges leading to initiation of a jet discharge between the upper positive layer and the screening charge layer at $t \sim 62$ s. Sudden jumps in the curves correspond to occurrence of IC discharges unless marked otherwise.

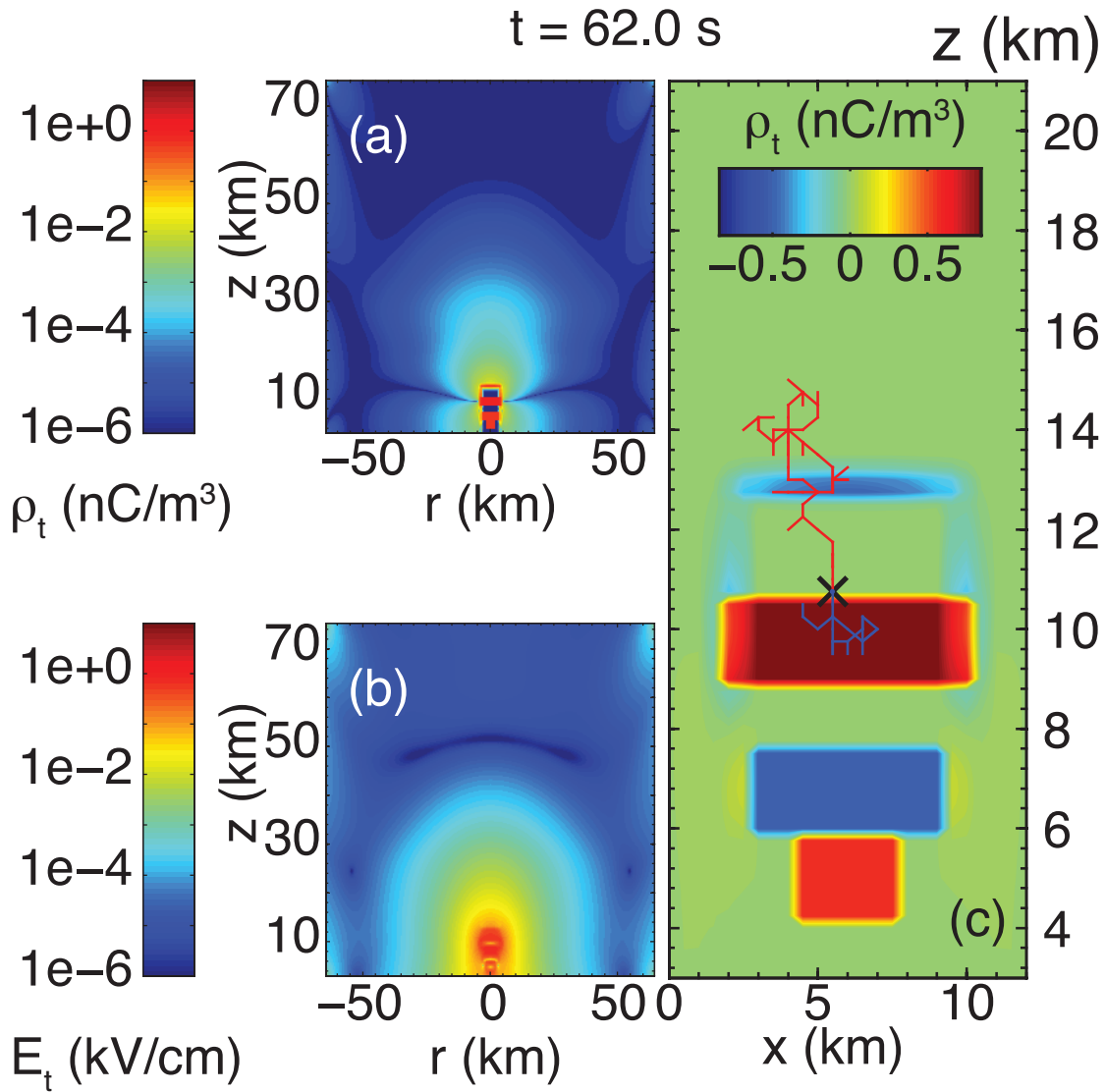


Figure 3. Total charge density (a) and electric field magnitude (b) at the moment of the jet initiation $t \sim 62$ s (see Figure 2). At this instant the electric field exceeds the lightning initiation threshold near the cloud upper boundary leading to an upward positive discharge (marked as +BJ in Figure 2). (c) Modeling of the jet discharge using the 3-D model, with charge densities as background.